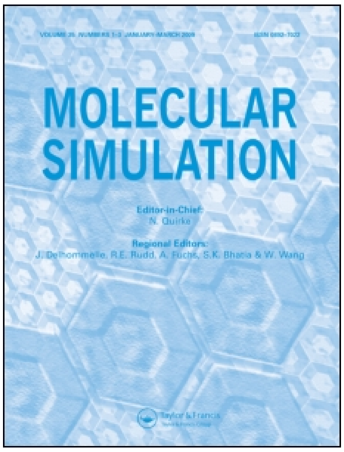

Molecular Simulation
Publication details, including instructions for authors and subscription information:
http://www.informaworld.com/smpp/title~content=t713644482

Molecular dynamics calculations of solid C_{60} under high pressure

Y. Kita[a]; I. Okada[a]
[a] Graduate School of Integrated Science, Yokohama City University, Yokohama, Japan

To cite this Article Kita, Y. and Okada, I.(2007) 'Molecular dynamics calculations of solid C_{60} under high pressure', Molecular Simulation, 33: 1, 165 — 169
To link to this Article: DOI: 10.1080/08927020601075329
URL: http://dx.doi.org/10.1080/08927020601075329

Molecular Simulation, Vol. 33, Nos. 1–2, 15 January–15 February 2007, 165–169

Molecular dynamics calculations of solid C_{60} under high pressure

Y. KITA* and I. OKADA

Graduate School of Integrated Science, Yokohama City University, 22-2 Seto, Kanazawa-ku, Yokohama 236-0027, Japan

(Received 31 July 2006; in final form 19 October 2006)

Recently, we have proposed the new intermolecular interaction model of C_{60}. Using this new model, we have analyzed the molecular rotational motions of C_{60} in solid state with the constant-temperature and constant-pressure molecular dynamics method at the temperature regions 180–340 K under the pressure regions 100–500 MPa. By analyzing the density of states of the molecular rotational motions, we found that the orientational phase transitions which involve the slightly volume change of the C_{60} crystal, are induced at 260 ∼ 280 K under 100 MPa, 280 ∼ 300 K under 200 MPa, 300 ∼ 320 K under 300 MPa and 320 ∼ 340 K under 400 MPa. The temperature/pressure variations of the order parameter also shows that C_{60} molecules rotate rapidly even below the orientational phase transition temperature.

Keywords: Fullerene; Molecular dynamics; High pressure; Phase transition

1. Introduction

C_{60} molecules have the nearly spherical shape of a truncated icosahedron [1], vertices of which are occupied with equivalent carbon atoms having a shorter "double"("DB") bond and two longer "single"("SB") bonds. The DB's fuse two slightly distorted hexagons and the SB's fuse a hexagon to a pentagon. At $T_C \simeq 260$ K under ambient pressure, it has been observed experimentally that the solid C_{60} undergoes a first-order phase transition in which the C_{60} molecules develop long-range orientational order between the molecules [2]. It has also been revealed experimentally that the transition temperature shifts upward with increasing pressure [3]. In both the orientationally disordered ($> T_C$) and ordered ($< T_C$) phases, the molecular centers of mass form a face-centered-cubic (fcc) lattice. In the high-temperature phase (space group $Fm\bar{3}m$), C_{60} crystals form plastic crystals [2], which the molecular centers of mass have a long range order, whereas the molecules are reorientating very rapidly. High resolution X-ray as well as neutron diffraction experiments, however, have shown a tendency occupying preferred orientations of molecules [4,5], and the X-ray diffuse scattering has indicated short-range orientational correlations [6], even in the $Fm\bar{3}m$ phase. The molecular reorientational motions, therefore, are not completely free. On the other hands, in the low-temperature phase (space group $Pa\bar{3}$), the C_{60} molecules have a long range orientational order, and then the crystal structure has been belonged to a simple-cubic (sc) with four orientationally non-equivalent molecules per unit cell [7]. The molecular stable orientations, found experimentally in the $Pa\bar{3}$ phase, are obtained by rotating four molecules at (000), $(\frac{1}{2}\frac{1}{2}0)$, $(0\frac{1}{2}\frac{1}{2})$ and $(\frac{1}{2}0\frac{1}{2})$ in the unit cell, which are oriented at a same standard orientation originally, by a setting angle ϕ around the local $\langle 111\rangle$, $\langle 1\bar{1}\bar{1}\rangle$, $\langle \bar{1}1\bar{1}\rangle$ and $\langle \bar{1}\bar{1}1\rangle$ axis, respectively [8]. The standard orientation is a molecular orientation introduced for convenience, in which the C_{60} molecule is oriented as the molecular twofold axes are aligned parallel to the cube edges being crystalline axes; there are two ways of setting standard orientation (A and B) [9]. By analyzing the neutron powder-diffraction profile, David *et al.* [7,10] has been suggested that the majority molecular orientation at the low temperature phase (P-orientation) is represented by the setting angle $\phi_P \simeq 22^\circ$ with the use of the standard orientation A, and whereas the minority orientation (H-orientation) finds itself in the setting angle $\phi_H \simeq 82^\circ$; the P- and H-orientations are described by $\phi_P \simeq 98^\circ$ and $\phi_H \simeq 38^\circ$ with the standard orientation B. In the most stable state in the $Pa\bar{3}$ phase in which all molecules are oriented to the P-orientation (pure P-phase), a molecular pentagon and a DB face each other (P-configuration)

*Corresponding author. Email: s045904f@yokohama-cu.ac.jp

Molecular Simulation
ISSN 0892-7022 print/ISSN 1029-0435 online © 2007 Taylor & Francis
http://www.tandf.co.uk/journals
DOI: 10.1080/08927020601075329

between all the nearest neighbor molecules. In a pure *H*-phase in which all molecules are oriented to the *H*-orientation, a molecular hexagon and a DB face almost each other (*H*-configuration) between all the nearest neighbor molecules with slightly higher energy. It has been found experimentally that the *P*-(*H*)orientation occupancy decreases (increases) with increasing temperature [7] and/or pressure [11]; the both orientations co-exist with each other below T_c. Under the ambient pressure, the energy difference between *P*- and *H*-orientations is estimated experimentally to be $\simeq 11\,\mathrm{meV}$ as the average value in the temperature range of 85–260 K [10,12]. Another orientational feature, in further lower temperature region, has been observed as a glass transition at $T_g \simeq 85\,\mathrm{K}$ [7]. Below T_g, the molecular reorientations are frozen due to the high energy barrier [13,14] 235–290 meV, and then the fractions of these molecular orientations remains practically constant.

It has been predicted experimentally that a thermally activated jumps of C_{60} molecules are induced between the two orientations [12], but the molecular rotational motions in crystals are not clarified in detail due to the difficulty in observing molecular rotations in bulk crystals. For the purpose of revealing the rotational motions and the orientational properties of C_{60} molecules in crystals, a great number of researchers has been proposed the empirical models for the intermolecular interaction of C_{60} [15]. In the earliest research, Cheng and Klein [16] have proposed a simple Lennard-Jones (12-6) model for C_{60} based on an atom–atom intermolecular potential technique. The models with the additional van der Waals interaction points has been proposed by Sprik *et al.* [17] The models with the effective Coulomb interactions between C_{60} molecules have been also developed by Lu *et al.* [18] and Pintschovius and Chaplot [19]. Lamoen and Michel [20] have presented the intermolecular interaction model based on Born–Mayer repulsion, van der Waals attraction and electrostatic multiples, in which the intermolecular interaction potential is expanded by the rotator function [21]. Their interaction models bring about success to revealing the orientational properties of C_{60} molecules in crystals qualitatively, but they are not enough quantitatively for reproducing the molecular orientational properties such as the energy difference and the activation energy between the *P*- and *H*-orientations. On the other hands, Savin *et al.* [22] has proposed the semi-empirical model for the intermolecular interaction of C_{60}, in which the Coulomb interaction is treated microscopically using molecular charge distributions estimated by the density functional theory (DFT) with the local-density approximation (LDA), and the short-range part of the intermolecular interaction is modeled by Lennard–Jones 12-6 interactions between the centers, delocalized over the surfaces of C_{60} molecules. Although their semi-empirical model has the quantitative accuracy for the orientational properties of C_{60} molecules in crystals, their model has not been applied to the molecular dynamics calculation and the relaxation calculations for the large systems, because of a great amount of computational costs in using their model. On the other hands, Hasegawa *et al.* [23] has performed the *ab initio* calculations, based on DFT with LDA, of C_{60} crystals. The intermolecular potential obtained by their calculation, however, is much shallower than that expected from the experimental heat of sublimation [24] due to the limited capability of the density-functional calculations to incorporate appropriately the effect of electron correlations at large separation. In addition, the performing *ab initio* calculations for the large systems has the difficulties as in the case of applying Savin's model to such systems.

Recently, we have proposed the new intermolecular interaction model of C_{60}, and have verified the validity of our model for describing the orientational properties of C_{60} in crystals [25,26]. In this paper, we will report the temperature and pressure dependency of the crystallographic properties of the solid C_{60} obtained by our simulations with the constant-temperature and constant-pressure technique in the molecular dynamics method.

2. Method

2.1 Anisotropic vdW model

The intermolecular interaction potential, used in this study, between molecule I and J [V_{IJ}] is expressed as the following form:

$$V_{\mathrm{IJ}} = \sum_{i,j}\left[\frac{6d_0}{\lambda-6}\exp\left\{-\frac{\lambda}{r_0}\left(R_{ij}^{\mathrm{IJ}}-r_0\right)\right\}-\frac{\lambda d_0}{\lambda-6}\left(\frac{r_0}{r_{ij}^{\mathrm{IJ}}}\right)^6 + \frac{1}{4\pi\varepsilon_0}\left\{\frac{\mathbf{D}_i^{\mathrm{I}}\cdot\mathbf{D}_j^{\mathrm{J}}}{r_{ij}^{\mathrm{IJ}^3}}-\frac{3\left(\mathbf{r}_{ij}^{\mathrm{IJ}}\cdot\mathbf{D}_i^{\mathrm{I}}\right)\left(\mathbf{r}_{ij}^{\mathrm{IJ}}\cdot\mathbf{D}_j^{\mathrm{J}}\right)}{r_{ij}^{\mathrm{IJ}^5}}\right\}\right],$$

where, $\mathbf{r}_{ij}^{\mathrm{IJ}} \equiv \mathbf{r}_i^{\mathrm{I}} - \mathbf{r}_j^{\mathrm{J}}$ is the radius vector directed from *j*th atom on molecule J toward *i*th atom on molecule I, $\mathbf{r}_{ij}^{\mathrm{IJ}}$ is the norm of $\mathbf{r}_{ij}^{\mathrm{IJ}}$, and R_{ij}^{IJ} is the 'anisotropic' atom–atom distance defined as

$$\begin{aligned} &R_{ij}^{\mathrm{IJ}}\left(\mathbf{r}_{ij}^{\mathrm{IJ}},\ \mathbf{a}_i^{\mathrm{I}},\ \mathbf{a}_j^{\mathrm{J}},\ \mathbf{b}_i^{\mathrm{I}},\ \mathbf{b}_j^{\mathrm{J}},\ \mathbf{c}_i^{\mathrm{I}},\ \mathbf{c}_j^{\mathrm{J}}\right) \\ &\quad = r_{ij}^{\mathrm{IJ}}\left\{1+f\left(\mathbf{e}_{ij}^{\mathrm{IJ}},\ \mathbf{a}_i^{\mathrm{I}},\ \mathbf{a}_j^{\mathrm{J}},\ \mathbf{b}_i^{\mathrm{I}},\ \mathbf{b}_j^{\mathrm{J}},\ \mathbf{c}_i^{\mathrm{I}},\ \mathbf{c}_j^{\mathrm{J}}\right)\right\}, \end{aligned} \tag{1}$$

where

$$\begin{aligned} &f\left(\mathbf{e}_{ij}^{\mathrm{IJ}},\ \mathbf{a}_i^{\mathrm{I}},\ \mathbf{a}_j^{\mathrm{J}},\ \mathbf{b}_i^{\mathrm{I}},\ \mathbf{b}_j^{\mathrm{J}},\ \mathbf{c}_i^{\mathrm{I}},\ \mathbf{c}_j^{\mathrm{J}}\right) \\ &= \alpha\left[\left(1-\mathbf{a}_i^{\mathrm{I}}\cdot\mathbf{e}_{ij}^{\mathrm{IJ}}\right)^3+\left(1+\mathbf{a}_j^{\mathrm{J}}\cdot\mathbf{e}_{ij}^{\mathrm{IJ}}\right)^3\right] \\ &\quad + \beta\left[-\left(\mathbf{a}_i^{\mathrm{I}}\cdot\mathbf{e}_{ij}^{\mathrm{IJ}}\right)^3-\left|\mathbf{a}_i^{\mathrm{I}}\cdot\mathbf{e}_{ij}^{\mathrm{IJ}}\right|^3+\left(\mathbf{a}_j^{\mathrm{J}}\cdot\mathbf{e}_{ij}^{\mathrm{IJ}}\right)^3-\left|\mathbf{a}_j^{\mathrm{J}}\cdot\mathbf{e}_{ij}^{\mathrm{IJ}}\right|^3\right] \\ &\quad + \gamma\left[-\left(\mathbf{b}_i^{\mathrm{I}}\cdot\mathbf{e}_{ij}^{\mathrm{IJ}}\right)^3-\left|\mathbf{b}_i^{\mathrm{I}}\cdot\mathbf{e}_{ij}^{\mathrm{IJ}}\right|^3+\left(\mathbf{b}_j^{\mathrm{J}}\cdot\mathbf{e}_{ij}^{\mathrm{IJ}}\right)^3-\left|\mathbf{b}_j^{\mathrm{J}}\cdot\mathbf{e}_{ij}^{\mathrm{IJ}}\right|^3 \right. \\ &\quad \left. -\left(\mathbf{c}_i^{\mathrm{I}}\cdot\mathbf{e}_{ij}^{\mathrm{IJ}}\right)^3-\left|\mathbf{c}_i^{\mathrm{I}}\cdot\mathbf{e}_{ij}^{\mathrm{IJ}}\right|^3+\left(\mathbf{c}_j^{\mathrm{J}}\cdot\mathbf{e}_{ij}^{\mathrm{IJ}}\right)^3-\left|\mathbf{c}_j^{\mathrm{J}}\cdot\mathbf{e}_{ij}^{\mathrm{IJ}}\right|^3\right], \end{aligned} \tag{2}$$

in which $\mathbf{a}_i^{\mathrm{I}}$, $\mathbf{b}_i^{\mathrm{I}}$, and $\mathbf{c}_i^{\mathrm{I}}$ are the unit vectors parallel to the "double" bond and two "single" bonds of ith atom on molecule I, respectively. $\mathbf{e}_{ij}^{\mathrm{IJ}}$ is the unit vector parallel to $\mathbf{r}_{ij}^{\mathrm{IJ}}$. The r_0, d_0, λ, α, β, γ, and η are fitting parameters. The first and second terms, in equation (1), are the Buckingham(exp-6) potential with an anisotropy in the repulsive term, which depends on not only the atom–atom distance but also the bond directions of each atoms, that is, the molecular orientations of molecules I and J. The third term in equation (1) is a dipole–dipole interaction in which permanent dipole moments are placed on carbon atoms and oriented parallel to 'double' bonds. Further details of our model are discussed in Ref. [26]

2.2 Molecular dynamics calculations of solid C_{60}

Molecular dynamics (MD) calculations were performed with the rigid body approximation for C_{60} at the temperature of 180, 200, 220, 240, 260, 280, 300, 320 and 340 K under 100, 200, 300, 400, and 500 MPa. The all molecular dynamics calculations were performed on the system with $4 \times 4 \times 4$ fcc unit cells, where 256 C_{60} molecules are contained, and with the three dimensional periodic boundary condition under the constant-temperature [T], thermodynamics tension [t] and the number of particles [N] (*TtN* statistical ensemble). We also employed the constant-temperature [27] and constant-pressure technique [28,29], which allows volume and shape fluctuations of the parallelepiped MD cell, and scales the translational and angular velocities of molecules using a heatbath variable. The required Nose and Ray–Rahman equations of motion for the molecular translational degrees of freedom were integrated by using a fifth-order Gear predictor–corrector algorithm [30]. The Euler equations for the molecular rotational degrees of freedom, described by quaternions, were integrated by a forth-order algorithm. To integrate these equations of motion, we used the most stable molecular configuration in solid state as initial coordinates. For all MD calculations, we simulated the systems for 200 ps with the time step of 2 fs. Typically, the systems needs the simulation time of $\simeq$20 ps for relaxing the temperature and lattice parameters of the systems. Thus, we analyzed the molecular and crystallographic properties with the calculation results after $\simeq$20 ps.

3. Results and discussions

Figure 1 shows the density of states for the translational(phonon) and rotational(libron) motions, obtained by the Fourier transformation of the autocorrelation functions of the molecular velocity and angular velocity averaged over simulation time and molecules. From figure 1, it is clearly found that the density of states of phonons, under any setting pressure, depends on the temperature slightly, and the spectrum is distributed from 20–70 cm^{-1}. On the other hands, the density of states of librons has the drastic change depending on the temperature; the libron peaks are not split and shift downward at the high temperature regions in contrast to the distributions at the low temperature regions. Such drastic changes implies the orientational phase transition of C_{60} molecules [26,31]. The phase transition temperatures [T_{C}] estimated from figure 1 are 260 $\sim$ 280 K under 100 MPa, 280 $\sim$ 300 K under 200 MPa, 300 $\sim$ 320 K under 300 MPa and 320 $\sim$ 340 K under 400 MPa. The orientational phase transition under 500 MPa was not observed at the setting temperatures in this study. It is also observed that the orientational phase transition involves the slightly volume change of the C_{60} crystal shown in figure 2, where T_{C} shifts upward with increasing pressure. In addition, our phase transition temperature of 300 $\sim$ 320 K under 300 MPa, is in good agreement with the results by the single-crystal neutron diffraction [11].

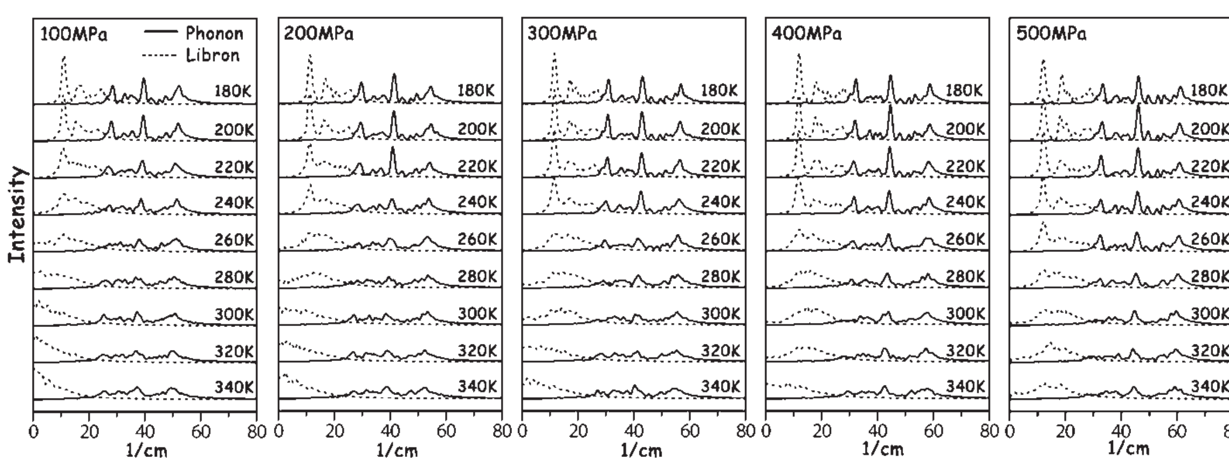

Figure 1. The calculated power spectra of the molecular translational (phonon) and librational (libron) motions in our simulation. Black and dotted curves are the density of states for the phonon and libron, respectively.

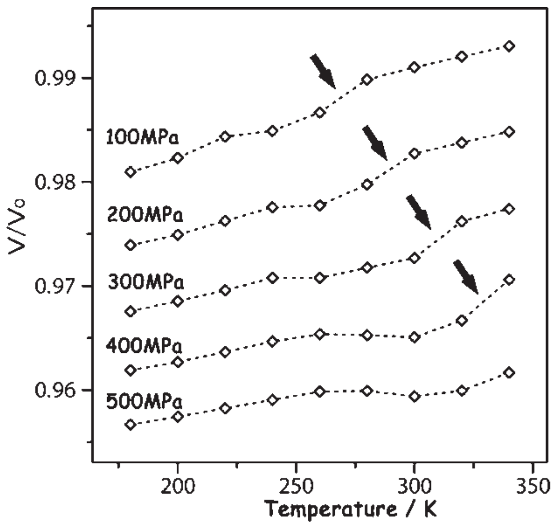

Figure 2. The temperature variation of the relative volume V/V_0 (V_0: the volume at 300 K under ambient pressure).

For analyzing the molecular rotational properties in detail, we also show the temperature variation of the order parameter in figure 3, proposed by Cheng and Klein [31]. Their order parameter is the auxiliary function defined by $Q_{6m} \equiv \sum Y_{6m}$ where Y_{6m} is the spherical harmonic function of sixth order which are defined clearly in Ref. [31] and $\sum$ is over all carbon atoms on the C_{60}. It is known that such auxiliary function takes a small value for the rapid molecular rotating, and a relatively large value for the "stopped" molecular rotating. From figure 3, it is found that the values of $\langle [Q_{6m}] \rangle$ are small considerably at the high temperature region, which means the rapid rotational motion of C_{60}. Furthermore, figure 3 indicates that C_{60} molecules rotate rapidly even below the orientational phase transition temperature estimated by analyzing the density of states of the librons.

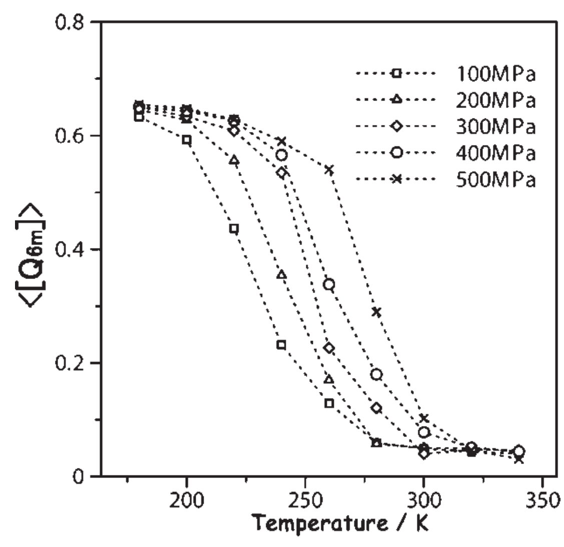

Figure 3. The temperature variations of the order parameter $\langle [Q_{6m}] \rangle$ for $m = 3$, which defined in Ref. [31].

4. Conclusion

In this study, we performed the theoretical analysis on solid C_{60} using the constant-temperature and constant-pressure molecular dynamics method with the new intermolecular interaction model of C_{60} proposed by us. By analyzing the temperature/pressure variations of the density of states of librons in solid C_{60}, we found that the orientational phase transition temperature are 260 $\sim$ 280 K under 100 MPa, 280 $\sim$ 300 K under 200 MPa, 300 $\sim$ 320 K under 300 MPa and 320 $\sim$ 340 K under 400 MPa. The temperature/pressure variations of the order parameter also shows that C_{60} molecules rotate rapidly even below the orientational phase transition temperature estimated by analyzing the density of states of the molecular librational motions.

References

[1] H.W. Kroto, J.R. Heath, S.C. O'Brien, R.F. Curl, R.E. Smalley. C_{60}: buckminsterfullerene. *Nature*, **318**, 162 (1985).
[2] P.A. Heiney, J.E. Fischer, A.R. McGhie, W.J. Romanow, A.M. Denenstein, J.P. McCauley Jr, A.B. Smith, D.E. Cox. Orientational ordering transition in solid C_{60}. *Phys. Rev. Lett.*, **66**, 2911 (1991).
[3] G.A. Samara, L.V. Hansen, R.A. Assink, B. Morosin, J.E. Schirber, D. Loy. Effects of pressure and ambient species on the orientational ordering in solid C_{60}. *Phys. Rev. B*, **47**, 4756 (1993).
[4] P.C. Chow, X. Jiang, G. Reiter, P. Wochner, S.C. Moss, J.D. Axe, J.C. Hanson, R.K. McMullan, R.L. Meng, C.W. Chu. Synchrotron x-ray study of orientational order in single crystal C_{60} at room temperature. *Phys. Rev. Lett.*, **69**, 2943 (1992).
[5] P. Schiebel, K. Wulf, W. Prandl, G. Heger, R. Papoular, W. Paulus. Orientationa disorder, the orientational density distribution and the rotational potential in C_{60}. *Acta Cryst.*, **A52**, 176 (1996).
[6] P. Launois, S. Ravy, R. Moret. Diffuse scattering and orientational correlations in solid C_{60}. *Phys. Rev. B*, **52**, 5414 (1995).
[7] W.I.F. David, R.M. Ibberson, T.J.S. Dennis, J.P. Hare, K. Prassides. Structural phase transitions in the fullerene C_{60}. *Europhys. Lett.*, **18**, 219 (1992).
[8] A.B. Harris, R. Sachidanandam. Orientational ordering of icosahedra in solid C_{60}. *Phys. Rev. B*, **46**, 4944 (1992).
[9] M.S. Dresselhaus, G. Dresselhaus, P.C. Eklund. *Science of Fullerenes and Carbon Nanotubes*, Academic Press, San Diego, CA (1996).
[10] W.I.F. David, R.M. Ibberson, T. Matsuo. High resolution neutron powder diffraction: a case study of the structure of C_{60}. *Proc. R. Soc. Lond. A*, **442**, 129 (1993).
[11] L. Pintschovius, O. Blaschko, G. Krexner, N. Pyka. Bulk modulus of C_{60} studied by single-crystal neutron diffraction. *Phys. Rev. B*, **59**, 11020 (1999).
[12] K. Prassides. Neutron scattering and μSR studies of fullerenes and their derivatives. *Phys. Scr.*, **T49**, 735 (1993).
[13] R.C. Yu, N. Tea, M.B. Salamon, D. Lorents, R. Malhotra. Thermal conductivity of single crystal C_{60}. *Phys. Rev. Lett.*, **68**, 2050 (1992).
[14] X.D. Shi, A.R. Kortan, J.M. Williams, A.M. Kini, B.M. Savall, M. Chaikin. Sound velocity and attenuation in single-crystal C_{60}. *Phys. Rev. Lett.*, **68**, 827 (1992).
[15] P. Launois, S. Ravy, R. Moret. Tests of current models of intermolecular potentials against X-ray diffuse scattering in C_{60}. *Phys. Rev. B*, **55**, 2651 and references therein (1997).
[16] A. Cheng, M.L. Klein. Molecular dynamics simulations of solid buckminsterfullerenes. *J. Phys. Chem.*, **95**, 6750 (1991).
[17] M. Sprik, A. Cheng, M.L. Klein. Modeling the orientational ordering transition in solid fullerene (C_{60}). *J. Phys. Chem.*, **96**, 2027 (1992).
[18] J.P. Lu, X.P. Li, R.M. Martin. Ground state and phase transitions in solid C_{60}. *Phys. Rev. Lett.*, **68**, 1551 (1992).
[19] L. Pintschovius, S.L. Chaplot. Neutron scattering study of the intermolecular vibrations in solid C_{60}. *Z. Phys. B*, **98**, 527 (1995).

[20] D. Lamoen, K.H. Michel. Crystal field, orientational order, and lattice contraction in solid C_{60}. *J. Chem. Phys.*, **101**, 1435 (1994).

[21] K.H. Michel, J.R.D. Copley, D.A. Neumann. Microscopic theory of orientational disorder and the orientational phase transition in solid C_{60}. *Phys. Rev. Lett.*, **68**, 2929 (1992).

[22] S. Savin, A.B. Harris, T. Yildirim. Towards a microscopic approach to the intermolecular interaction in solid C_{60}. *Phys. Rev. B*, **55**, 14182 (1997).

[23] M. Hasegawa, K. Nishidate, M. Katayama, T. Inaoka. Intermolecular potential and the equation of state of solid C_{60}. *J. Chem. Phys.*, **119**, 1386 (2003).

[24] C. Pan, M.P. Sampson, Y. Chai, R.H. Hauge, J.L. Margrave. The heats of sublimation of C_{60} and C_{70} from a polycrystalline mixture of C_{60} and C_{70}. *J. Phys. Chem.*, **95**, 2944 (1991).

[25] Y. Kita, K. Wako, I. Okada, M. Tachikawa. *Ab Initio* calculations of intermolecular interaction potentials of fullerene-fragments systems. *J. Theor. Comp. Chem.*, **4**, 49 (2005).

[26] Y. Kita, K. Wako, H. Goto, T. Naito, H. Kawai, I. Okada. Study on the intermolecular interaction of C_{60} and simulations on the orientational properties of C_{60} in crystals. *J. Chem. Phys.*, **125**, 034506 (2006).

[27] S. Nose. A unified formulation of the constant temperature molecular dynamics methods. *J. Chem. Phys.*, **81**, 511 (1984).

[28] J.R. Ray, A. Rahman. Statistical ensembles and molecular dynamics studies of anisotropic solids. *J. Chem. Phys.*, **80**, 4423 (1984).

[29] J.R. Ray, A. Rahman. Statistical ensembles and molecular dynamics studies of anisotropic solids. II. *J. Chem. Phys.*, **82**, 4243 (1985).

[30] C.W. Gear. *Numerical Initial Value Problems in Ordinary Differential Equations*, Prentice-Hall, Englewood Cliffs, NJ (1971).

[31] A. Cheng, M.L. Klein. Molecular-dynamics investigation of orientational freezing in solid C_{60}. *Phys. Rev. B*, **45**, 1889 (1992).